ARTICLE

Polyelectrolyte Multilayered Nanofilms as a Novel Approach for the Protection of Hydrogen Storage Materials

T. N. Borodina,* D. O. Grigoriev, D. V. Andreeva, H. Möhwald, and D. G. Shchukin

Max-Planck-Institute of Colloids and Interfaces, Research Campus Golm, 14424 Potsdam-Golm, Germany

ABSTRACT This work describes the encapsulation of hydrogen storage materials from organic solvents. Due to complex formation the shell provides stability and selective permeability. Specifically, sodium borohydride particles were encapsulated within polymer films by the layer-by-layer self-assembly of oppositely charged polyelectrolytes (polyethyleneimine and poly(acrylonitrile-co-butadiene-co-acrylic acid)). The polymer nanofilm fabrication was performed using dichloromethane as a working media. IR spectroscopy was applied to investigate the chemical interaction between the polyelectrolytes. The multilayer film preparation was verified by *Z*-potential measurements, scanning electron microscopy, and confocal laser microscopy. The stability of sodium borohydride protected with a polyelectrolyte shell was increased compared to that of the pure material under ambient conditions.

KEYWORDS: sodium borohydride • polyelectrolyte nanofilm • layer-by-layer self-assembly • protection

INTRODUCTION

Hydrogen storage is one of the most important tasks for a development of a hydrogen economy. Hydrogen is expected to play a key role in this area, especially in the transport sector (1). Interest in hydrogen as an alternative fuel has grown dramatically, due to its important properties such as low weight and high abundance. Moreover, oxidation products of hydrogen are environmentally benign. However, storage remains one of the most critical issues, which has to be solved before a technically and economically viable hydrogen economy can be established. In fact, a hydrogen economy will be difficult to achieve without effective storage systems.

Storing hydrogen is somewhat difficult, because of its low density and low critical temperature. Currently, there are a number of different approaches for hydrogen storage, including compressed or liquefied hydrogen in tanks (2), adsorption on activated carbon (3, 4) and carbon nanotubes (2−5), hydrogen-absorbing alloys (5, 6), inorganic hydrides including $NaBH_4$ (7, 8), NaH (9), LiH (10), $NaAlH_4$ (11), MgH_2 (12), $LiBH_4$ (13), and organic hydrogen-enriched compounds (methylcyclohexane, decalin) (14, 15).

Most research on hydrogen storage is focused on collecting hydrogen in a lightweight, compact manner for mobile applications. Classic high-pressure tanks have to be efficient and economical. However, physical storage by liquefaction or pressurization requires high-energy input and has to overcome associated safety risks (2). Zubizarreta et al. (16) demonstrated a series of commercial carbons with different structural and textural properties for hydrogen storage, but these materials were found to be ineffective, due to the fact that only a small fraction of the carbon surface interacts with hydrogen molecules under moderate conditions (17).

Recently, much attention has been paid to metal hydrides as a promising way to storing hydrogen. It was mentioned that the metal−hydrogen bond offers the advantage of very high density at moderate pressure and liberation of all stored hydrogen at the same pressure (2). Moreover, metal hydrides can easily bind and release hydrogen under optimum working conditions in order to be used as commercial fuels. $NaBH_4$ (SBH) has attracted a great deal of attention, due to a high theoretical hydrogen capacity (10.6 wt %) (18). The hydrogen in the $NaBH_4$ is located in the corners of a tetrahedron with boron in the center. The negative charge of the anion, $[BH_4]^-$, is compensated by the cation Na^+ (19). SBH is an interesting hydrogen storage material, since it is easy to handle compared with other hydrides and can be easily synthesized from common natural resources. However, the drawback of this material is that it spontaneously undergoes a decomposition reaction in air- and moisture-rich environments.

The main objective of the presented paper is the elaboration of effective protection for sensitive hydrogen storage materials by covering their surface with a multilayer nanofilm. Since the handling of such materials involves a great deal of restrictions, this causes specific challenges for their preparation:

- The preparation should not be performed in water but in organic solvents. Thus, the coating materials to be selected should be organically soluble.
- The materials should form a stable complex.
- The shell should be as impermeable as possible to polar compounds.

In view of this, the layer-by-layer (LbL) self-assembly technique is a promising method for the protective coating of hydrogen-enriched materials. Mainly the LbL adsorption

* To whom correspondence should be addressed. Tel: +49-(0)331-5679447. Fax: +49-(0)331-5679222. E-mail: tatiana.borodina@mpikg.mpg.de.
Received for review December 09, 2008 and accepted March 24, 2009

DOI: 10.1021/am8002236

Published on Web 04/21/2009

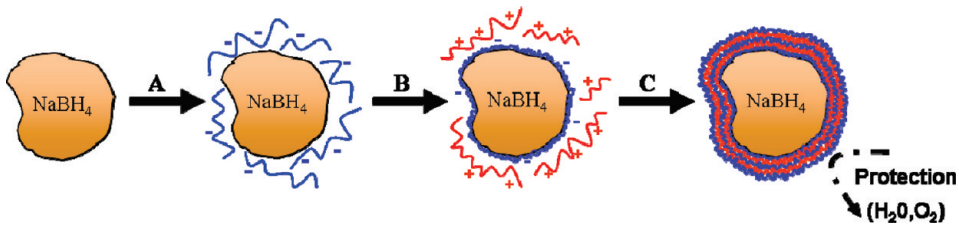

FIGURE 1. Scheme of the polyelectrolyte coating of sodium borohydride particles by layer-by-layer adsorption: (step A) polyanion adsorption; (step B) polycation adsorption; (step C) multilayer nanofilm formation.

is based on the electrostatic interaction between the oppositely charged polyelectrolytes, but hydrogen bonding, van der Waals interactions, charge-transfer interactions, and hydrophobic forces also make an important contribution to the multilayer film formation (20−23). Since the first report by Decher et al. (24), the LbL technique has been used for the preparation of optical or electrochemical devices, biosensors, separation membranes, catalytic and drug-delivery systems, etc. (21, 23, 25, 26). Until now, the application of this technique has been limited to the use of water-based solvents for nanofilm fabrication. Only a few studies have reported the assembly of polyelectrolytes from nonaqueous working media. Zhang et al. showed that formamide/water mixed solvent could be used for the LbL self-assembly of water-insoluble polyelectrolytes and investigated the influences of solvent composition, solution properties, and charge density on this process (27). Tuo et al. used *N*,*N*-dimethylformamide for azo-polyelectrolyte multilayer film fabrication together with a polyelectrolyte aqueous solution (28). Kaminemi et al. and Dobbins et al. demonstrated the successful preparation of polymeric nanofilms using formamide as an alternative solvent for the dissolution of polystyrene sulfonate and polyallylamine hydrochloride (29, 30). They also showed the possibility of using such nanofilms for the protection of water-sensitive sodium aluminum hydride particles.

In this work, dichloromethane (DCM) was used as the solvent for performing LbL nanoassembly onto the surface of sodium borohydride (SBH) particles. Anhydrous DCM can dissolve polyelectrolytes to be deposited: polyethyleneimine (PEI) and poly(acrylonitrile-co-butadiene-co-acrylic acid) (PABA) as polycation and polyanion, respectively, which demonstrate the ability to form a polyelectrolyte complex in organic solvent. It was shown that microparticles of SBH coated with a polyelectrolyte shell are more stable in the open atmosphere as compared to the pristine SBH.

RESULTS AND DISCUSSION

Preparation of Coated Sodium Borohydride (SBH) Microparticles. The polymer multilayers are constructed on SBH by the rather simple experimental procedure sketched in Figure 1. If the process of nanofilm growth starts from a negatively charged polymer, the next adsorption layer is the polycation (positively charged). After each deposition step the particles have to be rinsed with the solvent in order to remove the polyelectrolytes (PE) which are not tightly bound to the surface. This ensures that no chemical interactions take place between polymers in the

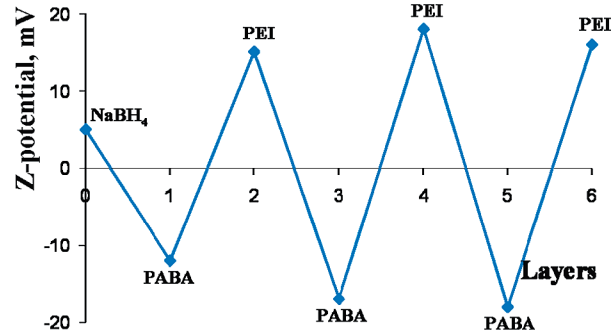

FIGURE 2. *Z* potential as a function of layer number for sodium borohydride particles coated with poly(acrylonitrile-co-butadiene-co-acrylic acid) and polyethyleneimine.

bulk solution during the next adsorption step. For the preparation of the microcontainers, SBH powder was dispersed in DCM. According to the scheme (Figure 1), PABA and PEI were adsorbed sequentially onto the surface of SBH particles (steps A and B). Finally, SBH particles were coated with three bilayers of PABA and PEI (step C). In this work, we used solutions of polyelectrolytes containing more polymer than was needed for the saturation adsorption and then removed the polymer excess by centrifugation and solvent washing.

The assembly of multilayers on SBH particles was monitored by measurements of the electrophoretic mobility (Figure 2). The *Z* potential of the initial SBH particles in DCM is positive. Therefore, the first layer has to be coated with a polyanion. The SBH particles coated with alternating layers of PABA and PEI yield an alternating *Z* potential of −18 mV (outer layer is PABA) to +18 mV (outer layer is PEI). These data demonstrate that the deposition of PABA is effective in reversing the sign of the surface charge when deposited alternately with a strong polyelectrolyte, PEI. *Z*-potential measurements were taken after each adsorption step, and the reversal of charge showed the growth of nanofilms on the SBH particles.

In order to prove whether the PEI/PABA multilayer reacts with SBH or not, X-ray diffraction (XRD) measurements were performed. The XRD patterns of untreated SBH before and after storage under outdoor conditions and SBH protected by the polyelectrolyte coating are shown in Figure 3. The peaks observed on the pattern of untreated SBH after storage correspond to the crystallinity of $NaB(OH)_4$ (circles), showing the hydrolysis of unprotected SBH upon reaction with environmental water (31). On the other hand, it is clearly seen that SBH coated with a PE multilayer has the same peaks as those of the crystalline structure of pristine SBH (Figure 3, triangles) (32). The absence of any changes in SBH

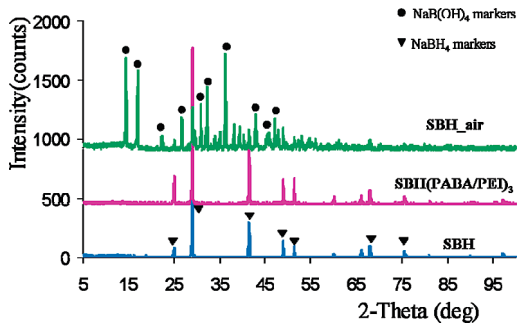

FIGURE 3. XRD patterns of pristine sodium borohydride (bottom curve), of the same substance after storing at the ambient conditions (upper curve), and of SBH coated with six layers of the polyelectrolytes (middle curve).

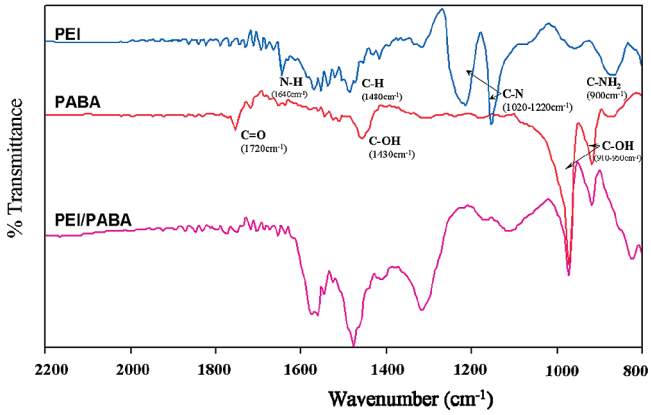

FIGURE 4. FTIR spectra of PEI film, PABA film, and PEI/PABA composite film.

crystallinity after adsorption of six PE layers allows us to consider that the PEI/PABA multilayer did not react with the core material (SBH). Any interactions between a first layer (polyanion PABA) and SBH would be immediately noticeable in the pattern of the coated SBH, and the observed opposite behavior confirms that the carboxylic functional groups of PABA had no influence on SBH.

FTIR spectroscopy was used to demonstrate the interaction between PEI and PABA in DCM. Figure 4 shows the spectra of PEI, PABA, and PEI/PABA films. The pure PEI exhibits a number of typical absorption features below 2000 cm^{-1} (33). The IR spectrum of the PEI film displays peaks at 1640 cm^{-1} (N−H stretch of primary amines), 1480 cm^{-1} (C−H bending vibration), and 1150−900 cm^{-1} (C−N stretching vibration). With regard to the spectrum of the PABA film, the absorption band at 1720 cm^{-1} is assigned to the C═O group. One band at 1430 cm^{-1} may be assigned to the O−H bend in the COOH groups. The strong bands at 910−950 cm^{-1} are ascribable to O−H vibrations (34). It can be seen that the spectrum of the PEI/PABA film has bands at 950 and 910 cm^{-1}, similar to the spectrum of pure PABA. In the spectrum of the PEI/PABA film the peak at 1720 cm^{-1} is not observed. Moreover, the peak at 1720 cm^{-1} is shifted probably to 1600 cm^{-1} due to the deprotonation of COOH. This demonstrates the complex formation between COO^- and NH^+ groups. A new broad band around 1100 cm^{-1} indicates the presence of intramolecular hydrogen bonding between PABA and PEI molecules (34). Moreover, the slight shift of the band at 1480 cm^{-1} to 1470 cm^{-1} may also be attributed to the formation of a stable complex between PABA and PEI.

To demonstrate the success of the nanofilm buildup, fluorescein isothiocyanate (FITC) was attached to PEI as a fluorescence label. Figure 5 shows typical confocal images of SBH particles coated with PABA and PABA/PEI-FITC. After deposition of first PABA layer on the SBH surface no fluorescence was observed (Figure 5A,B). On the other hand, an observable fluorescence is seen for the SBH particles coated with PEI-FITC in the next step, which illustrates the efficiency of the polyelectrolyte adsorption on the SBH particle surface (Figure 5 D). The success of the polyelectrolyte adsorption is also confirmed by comparison between transmission and fluorescence images (Figure 5C,D).

Additionally, the successful coating process is illustrated by SEM (Figure 6). The images reveal the surface morphology of SBH microparticles during the subsequent stages of the deposition process and demonstrate the formation of a progressively dense polyelectrolyte coating on the surface of SBH. During the subsequent polymer adsorption steps the porosity is gradually decreased (Figure 6A,C,E,G). Comparison between the pristine particles (Figure 6A,B) and samples coated with six PE layers (Figure 6G,H) shows the efficiency of the polymer deposition. As one can see, the cracks in the particles are covered more and more with the polyelectrolytes in the series Figure 6B−H. As a result, better protection of the metal hydride could be achieved due to blocking of the access to the SBH surface by the deposited polyelectrolyte multilayers.

We suggest that the novel nanofilms will weaken interactions between the metal hydride and the environment. The formed polyelectrolyte shell provides controlled release of hydrogen gas as well as controlled introduction of dopant species to the surface of the hydride particles; protection of hydrogen storage materials from air and moisture (Figure 1).

Test of Stability. In order to demonstrate the stability of the coated SBH particles, pure SBH and SBH/PABA/PEI obtained by the LbL technique were exposed to the atmosphere under room conditions (relative humidity 79%, 101 800 Pa, 22 °C). Figure 7 shows the images taken after 0, 4, 8, 10, and 12 h from the beginning of the storage. Unprotected SBH is degraded quickly, whereas PE-protected SBH remains almost stable. After 4 h, unprotected SBH started to react with moisture from the air. Evidently, after 12 h most of the unprotected SBH sample was completely destroyed. For SBH/PABA/PEI, visible changes do not appear even after 12 h.

To obtain a quantitative measure for SBH protection by PEs, the rate of weight increase of SBH during the storage was measured. SBH hydrolysis with subsequent $NaB(OH)_4$ formation explains the increase in sample weight. Figure 8 illustrates the weight increase of pristine and protected SBH. It is obvious that the stability of protected SBH is improved in comparison to that of unprotected material. In the case of untreated SBH, the relative weight increase over 24 h was

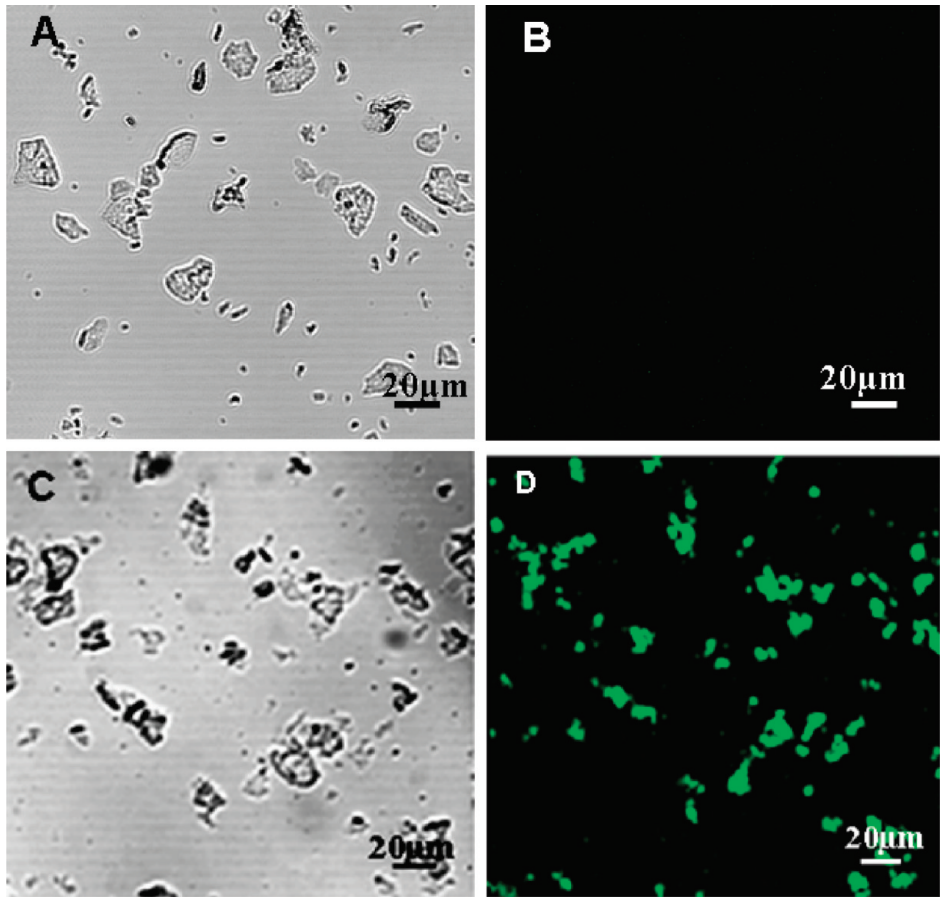

FIGURE 5. CLSM images of sodium borohydride particles coated with PABA (A and B) and PEI-FITC (C and D). Parts A and C are transmission images, and parts B and D are fluorescence images.

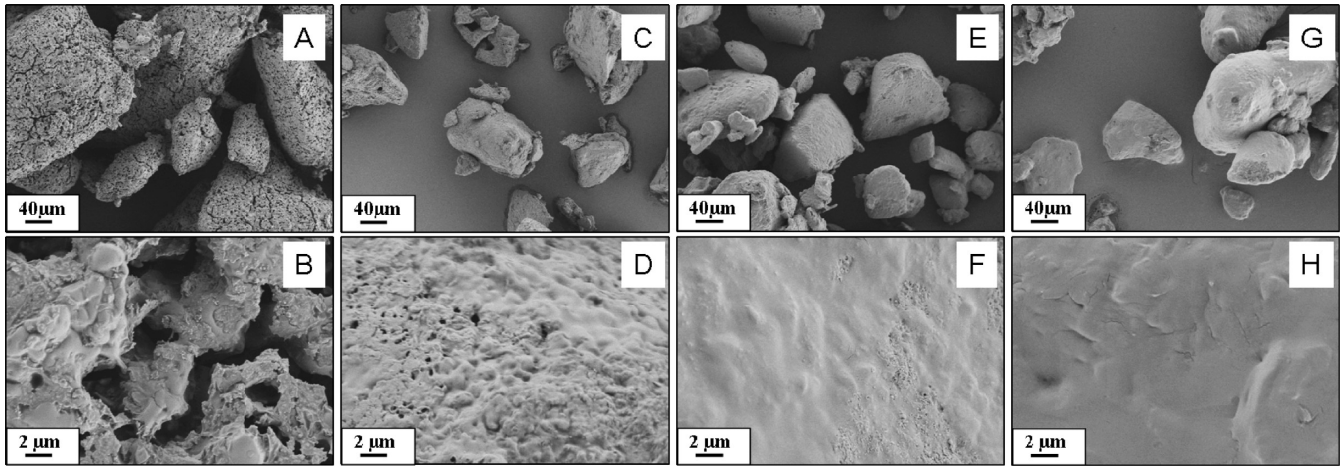

FIGURE 6. SEM images of pristine sodium borohydride particles (A,B) and particles coated with two (C, D), four (E, F) and six (G, H) layers of polyelectrolytes.

59%. For coated SBH, this amount was more than 2 times less. The results confirm the increased stability of SBH protected by a PE shell and the reduced interactions between SBH and the environment.

To study the temperature-dependent behavior of the polyelectrolyte PABA/PEI multilayer film, we performed measurements on the weight variation of SBH/PABA/PEI composites at 20, 40, and 80 °C. Equivalent amounts of protected SBH were kept at fixed temperatures over 12 h. Although for all three samples a weight increase effect was observed (Figure 9), an increase in temperature was accompanied by a reduction in the weight growth. Köhler et al. mentioned the heat-shrinkage effect for a few types of polyelectrolyte shells (35). They explained this as a result of temperature-enhanced gradual equilibration of the initially nonequilibrium PE shell accompanying by the higher mobility of shell-forming PEs and thickening and densification of shell walls. Our findings show that the heat-shrinkage effect

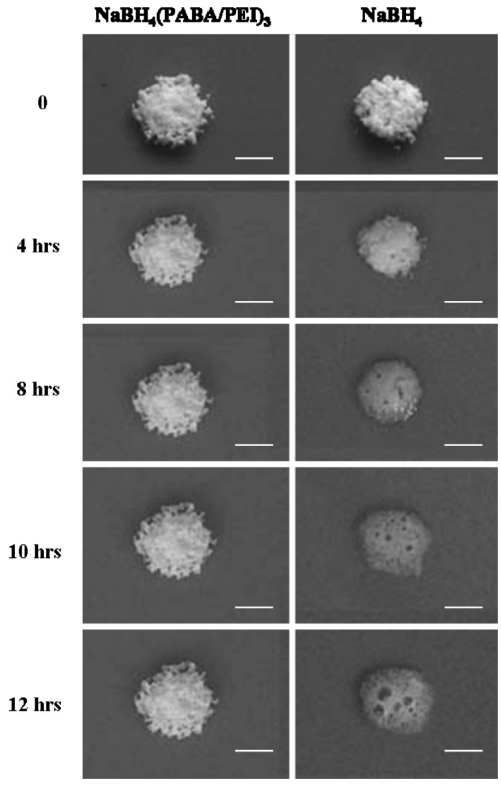

FIGURE 7. Photographs of protected and unprotected sodium borohydride particles during storage under ambient conditions. The samples were placed on the glass surface and exposed to the atmosphere. The images were taken by a photocamera (scale bar 1 cm).

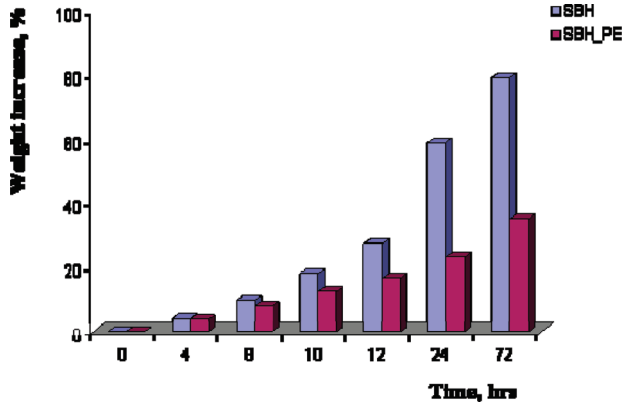

FIGURE 8. Relative weight increase (in percent) of the pristine and coated sodium borohydride during storage under ambient conditions.

is presented also in the case of the PABA/PEI polyelectrolyte complex, allowing the assumption that the stability of the PE coating increases at elevated temperatures. Then, an increase of temperature leads to better protection of SBH.

CONCLUSIONS

We developed a new protective coating for hydrogen storage materials prepared by the layer-by-layer technique. Dichloromethane was used as the solvent for polyelectrolyte dissolution and layer-by-layer assembly of the polyelectrolyte shell. SBH particles were successfully coated in nonaqueous media with polyethyleneimine and poly(acrylonitrile-co-butadiene-co-acrylic acid). The efficiency of the multilayer

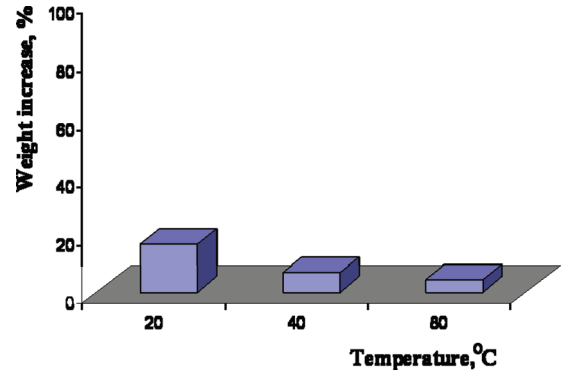

FIGURE 9. Relative weight increase (in percent) of coated sodium borohydride after 12 h storage at 20, 40, and 80 °C.

nanofilm fabrication on the surface of SBH and the complex formation between the polyelectrolytes were confirmed via measurements of the electrophoretic mobility, FTIR spectroscopy, XRD, CLSM, and SEM. The SBH/polyelectrolyte composite is more stable compared to unprotected SBH during storage in the open atmosphere. The polyelectrolyte shell protects water-sensitive metal hydrides against moisture and air. The demonstrated approach for hydride protection can find applications in hydrogen storage systems and could be used in hydrogen fuel cells.

EXPERIMENTAL SECTION

Materials. Sodium borohydride (SBH) powder (~30 μm), branched polyethyleneimine (PEI, MW ~10 000–25 000), poly(acrylonitrile-co-butadiene-co-acrylic acid) (acrylonitrile, ~18 wt %; PABA, MW ~3600), and dichloromethane (DCM, anhydrous) were purchased from Sigma-Aldrich and used without further purification.

Preparation of the Coated SBH. SBH powder was dispersed in DCM and used as template for the multilayer film formation. The solutions of polyelectrolytes were made in DCM with a concentration of 4 g L^{-1}. Multilayer films were grown by alternate incubation of SBH particles in solutions of polyanion (PABA) and polycation (PEI) at room temperature. SBH particles were intensively shaken for 15 min during each adsorption step. Excess polyelectrolyte was removed by centrifugation. Between each deposition step, SBH particles were washed with DCM. Thus, SBH particles coated with three bilayers of PABA/PEI were prepared. SBH was handled under inert conditions (using a glovebox and Schlenk system).

Electrophoretic Mobility. The *Z* potential of the coated containers was measured by a Zeta Sizer (Malvern Instruments). Each value was averaged from three measurements. The solvent used was DCM; therefore, the instrument settings were changed in order to account for the parameters of the solvent used, such as its viscosity, refractive index, and dielectric constant.

FTIR Spectroscopy. The substrates used for IR measurements were one-side polished (100) silicon wafers (ACM, France) cut into rectangles 3 cm by 1 cm. The wafers were first cleaned by treatment in hot piranha solution (H_2O_2 (35%)/H_2SO_4 (98%) 1/1 v/v) for 20 min and then thoroughly washed with deionized water. The cleaned wafers were dried with nitrogen gas.

The first layer was deposited by dipping the substrate into solutions of PEI in DCM for 20 min. Adsorption of PABA was made from a solution of polymer in DCM as a second layer. The substrate was rinsed by dipping three times with DCM and dried with a stream of nitrogen after the deposition of each polyelectrolyte.

Experiments were conducted on a Bruker Hyperion 2000 IR microscope equipped with a 15 × 8 IR objective and an MCT detector. To obtain the absorbance spectra analyzed below, each interferogram was normalized to the corresponding background of the silicon wafer substrate washed with DCM.

X-ray Diffraction. The crystalline structure of the sample was determined by a X-ray powder scattering diffractometer (Cu Kα =1.5418 Å) D8 Bruker.

Confocal Laser Scanning Microscopy (CLSM). Optical images of SBH microparticles were obtained using a Leica TCS SP confocal scanning system (Leica, Germany) equipped with a 10× dry and a 100× oil immersion objective (numerical aperture 0.3 and 1.4).

Scanning Electron Microscopy (SEM). SEM measurements were performed using a Gemini 1550 instrument at an operation voltage of 3 keV. The samples were prepared by placing a drop of the sample solution onto a glass substrate, followed by drying at room temperature and gold sputtering.

Acknowledgment. This work was supported by the EU NANOHy project (grant agreement 210092).

REFERENCES AND NOTES

(1) Satyapal, S.; Petrovic, J.; Read, C.; Thomas, G.; Ordaz, G. *Catal. Today* **2007**, *120* (3−4), 246–256.
(2) Schlapbach, L.; Züttel, A. *Nature (London)* **2001**, *414*, 353–358.
(3) Chanine, R.; Bose, T. K. *Int. J. Hydrogen Energy* **1994**, *19*, 161–164.
(4) Kojima, Y.; Suzuki, N. *Appl. Phys. Lett.* **2004**, *84*, 4113–4115.
(5) Dillon, A. C.; Jones, K. M.; Bekkedahl, T. A.; Kiang, C. H.; Bethune, D. S.; Heben, M. J. *Nature (London)* **1997**, *386*, 377–379.
(6) Tamura, T.; Tominaga, Y.; Matumoto, K.; Fuda, T.; Kuriiwa, T.; Kamegawa, A.; Takamura, H.; Okada, M. *J. Alloys Compd.* **2002**, *330/332*, 522–525.
(7) Schlesinger, H. I.; Brown, H. C.; Finhold, A. E.; Gilbreath, J. R.; Hoekstra, H. R.; Hyde, E. K. *J. Am. Chem. Soc.* **1953**, *75*, 215–219.
(8) Amendola, S. C.; Sharp-Goldman, S. L.; Janjua, M. S.; Kelly, M. T.; Petillo, P. J.; Binder, M. *J. Power Sources* **2000**, *85*, 186–189.
(9) DiPietro, J. P.; Skolnik, E. G. *Proceedings of the 2000 U.S. DOE Hydrogen Program Review*; San Ramon, California, Golden, Colorado; National Renewable Energy Laboratory, Vol. II, 2000; NREL/CP-570-28890.
(10) McClaine, A. W.; Breault, R. W.; Larsen, C.; Konduri, R.; Rolfe, J.; Becker, F.; Miskolczy, G. *Proceedings of the 2000 U.S. DOE Hydrogen Program Review*; San Ramon, California, Golden, Colorado; National Renewable Energy Laboratory, Vol. II, 2000; NREL/CP-570−28890.
(11) Bogdanovic, B.; Schwickardi, M. *J. Alloys Compd.* **1997**, *253/254*, 1–9.
(12) Kojima, Y.; Suzuki, K.; Kawai, Y. J. *Mater. Sci. Lett.* **2004**, *39*, 2227–2229.
(13) Kojima, Y.; Kawai, K.; Kimbara, M.; Nakanishi, H.; Matsumoto, S. *Int. J. Hydrogen Energy* **2004**, *29*, 1213–1217.
(14) Kojima, Y.; Kawai, K. *Chem. Commun.* **2004**, *19*, 2210–2211.
(15) Newson, E.; Haueter, Th.; Hottinger, P.; Von Roth., F.; Scherer, G. W. H.; Schucan, Th. N. *Int. J. Hydrogen Energy* **1998**, *23*, 905–909.
(16) Zubizarreta, L.; Gomez, E. I.; Arenillas, A.; Ania, C. O.; Parra, J. B.; Pis, J. J. *Adsorption* **2008**, *14*, 557–566.
(17) Becher, M.; Haluska, M.; Hirscher, M.; Quintel, A.; Skakalova, V.; Dettlaff-Weglikovska, U.; Chen, X.; Hulman, M.; Choi, Y.; Roth, S.; Meregalli, V.; Parrinello, M.; Ströbel, R.; Jörissen, L.; Kappes, M. M.; Fink, J.; Züttel, A.; Stepanek, I.; Bernier, P. *C. R. Phys.* **2003**, *4*, 1055–1062.
(18) Nijkamp, M. G.; Raaymakers, J. E. M. J.; van Dillen, A. J.; de Jong, K. P. *Appl. Phys. A: Mater. Sci. Process.* **2001**, *72*, 619–623.
(19) Züttel, A.; Rentsch, S.; Wenger, P.; Sudan, P.; Mauron, Ph.; Emmenegger, Ch. *Proc. Fabr. Adv. Mater. XI* **2002**, 107–122.
(20) Steitz, R.; Jaeger, W.; von Klitzing, R. *Langmuir* **2001**, *17*, 4471–4474.
(21) Stockton, W. B.; Rubner, M. F. *Macromolecules* **1997**, *30*, 2712–2716.
(22) Fu, Y.; Chen, H.; Qiu, D. L.; Wang, Z. Q.; Zhang, X. *Langmuir* **2002**, *18*, 4989–4995.
(23) Sukhishvili, S. A.; Granick, S. *Macromolecules* **2002**, *35*, 301–310.
(24) Decher, G.; Hong, J. D.; Schmitt, J. *Thin Solid Films* **1992**, *210*−*211*, 831–835.
(25) Shchukin, D. G.; Patel, A. A.; Sukhorukov, G. B.; Lvov, Y. M. *J. Am. Chem. Soc.* **2004**, *126*, 3374–3375.
(26) Zhang, H. Y.; Wang, D.; Wang, Z. Q.; Zhang, X. *Eur. Polym. J.* **2007**, *43*, 2784–2791.
(27) Zhang, P.; Qian, J. W.; An, Q. F.; Du, B. Y.; Liu, X. Q.; Zhao, Q. *Langmuir* **2008**, *24*, 2110–2117.
(28) Tuo, X.; Chen, D.; Cheng, H.; Wang, X. *Polym. Bull.* **2005**, *54*, 427–433.
(29) Kamineni, V. K.; Lvov, Y. M.; Dobbins, T. A. *Langmuir* **2007**, *23*, 7423–7427.
(30) Dobbins, T. A.; Kamineni, V.; Lvov, Y. M. *Mater. Matters* **2007**, *2* (2), 19–21.
(31) Kanturk, A.; Sari, M.; Piskin, S. *Korean J. Chem. Eng.* **2008**, *25* (6), 1331–1337.
(32) Varin, R. A.; Chiu, Ch. *J. Alloys Compd.* **2005**, *397*, 276–281.
(33) Lakard, S.; Herlem, G.; Lakard, B.; Fahys, B. *J. Mol. Struct. (THEOCHEM)* **2004**, *685*, 83–87.
(34) Shurvell, H. F. *Spectra-Structure Correlation* **2002**, 1783–1816.
(35) Köhler, K.; Sukhorukov, G. B. *Adv. Funct. Mater.* **2007**, *17*, 2053–2061.

AM8002236